Nonreciprocal Josephson Linear Response

Pauli Virtanen* and Tero T. Heikkilä†
Department of Physics and Nanoscience Center, University of Jyväskylä, P.O. Box 35 (YFL), FI-40014 University of Jyväskylä, Finland

(Received 28 June 2023; accepted 22 December 2023; published 22 January 2024)

We consider the finite-frequency response of multiterminal Josephson junctions and show how nonreciprocity in them can show up at linear response, in contrast to the static Josephson diodes featuring nonlinear nonreciprocity. At finite frequencies, the response contains dynamic contributions to the Josephson admittance, featuring the effects of Andreev bound state transitions along with Berry phase effects, and reflecting the breaking of the same symmetries as in Josephson diodes. We show that outside exact Andreev resonances, the junctions feature nonreciprocal reactive response. As a result, the microwave transmission through those systems is nondissipative, and the electromagnetic scattering can approach complete nonreciprocity. Besides providing information about the nature of the weak link energy levels, the nonreciprocity can be utilized to create nondissipative and small-scale on-chip circulators whose operation requires only rather small magnetic fields.

DOI: 10.1103/PhysRevLett.132.046002

Nonreciprocal superconducting electronics has been intensely studied in the recent years, as an important building block for future superconducting devices. Particular attention has been paid to Josephson diodes that feature different critical currents for two directions of supercurrent [1–13]. However, exploiting such nonreciprocity in high-speed electronics, for example, for rectification would require exciting the junction with a radio frequency signal whose amplitude exceeds smaller of the critical currents. This nonlinear regime may turn out cumbersome for many applications.

A natural question then to ask is under which conditions it might be possible to realize nonreciprocal response of Josephson junctions under linear response. At low frequencies, they are characterized by their inductive response, which is always reciprocal. It is hence necessary to go beyond the static regime. Moreover, any two-terminal system is bound to have reciprocal linear response.

In this Letter, we consider the generic finite-frequency linear response of multiterminal Josephson junctions. The dynamic features are connected with the subgap Andreev bound states (ABS) [14] in weak links with finite transmission. Therefore, we first discuss general aspects of the response of Andreev bound state systems, and then outline a minimal microscopic model. The results illustrate that significant nonreciprocal response is essentially always present if the system is flux biased. Moreover, we show that the φ_0 effect [15–17] that usually accompanies the superconducting diode effect also results to a nonreciprocal radio frequency response. Such nonreciprocity is reactive and occurs within a large bandwidth around the Andreev bound state resonances.

We also show how the nonreciprocity can be readily measured via the microwave scattering from the junction [see Fig. 1(a)]. In particular, it becomes possible to realize an Andreev bound state -based Josephson circulator, which has a small footprint, large bandwidth, and high ratio between "forward" and "reverse" circulation. Such systems may rival other recent suggestions for on-chip circulators, such as those based on conventional insulator-based Josephson junctions [18], or those based on mechanical resonators [19].

Linear response.—The electromagnetic linear response of a multiterminal system is characterized by its susceptibility χ_{ij}, which relates current J^i in each lead i to the driving by voltages V_j in other leads: $J^i(\omega) = \sum_j \chi_{ij}(\omega) V_j(\omega)/(-i\omega)$. The Kubo formula for the ABS susceptibility reads [20–22]

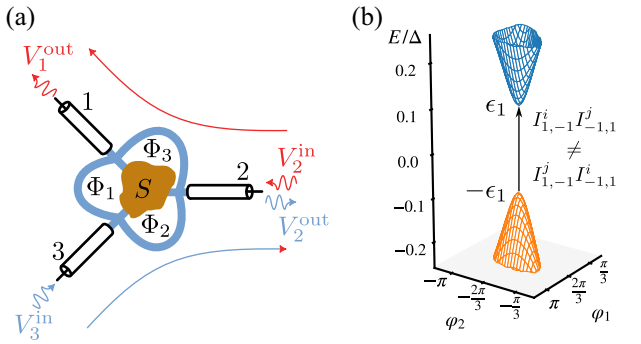

FIG. 1. (a) Nonreciprocal electromagnetic scattering parameter $\mathcal{S}_{ij} \neq \mathcal{S}_{ji}$, which relates rf signal inputs to outputs, $V_i^{\rm out} = \mathcal{S}_{ij} V_j^{\rm in}$. Its asymmetry originates from time-reversal breaking due to the electronic scattering matrix S, or external flux biasing Φ_i. (b) Transition involving the lowest Andreev bound state. Nonreciprocal response originates from nonsymmetric current operator matrix elements.

$$\chi_{ij}^{\mathrm{ABS}}(\omega) = 2\sum_{kk'} I^i_{kk'} I^j_{k'k} \frac{f_k - f_{k'}}{\epsilon_k - \epsilon_{k'} + \hbar\omega + i0^+}. \quad (1)$$

Here, the ABS $|k\rangle$ are at energies ϵ_k, with summations running over also negative energies. The states couple to the electromagnetic vector potential via current operators $\hat{J}^i$, with corresponding matrix elements $I^i_{kk'}$. Moreover $f_k = f(\epsilon_k) = 1/(e^{\epsilon_k/T}+1)$ is a Fermi function.

Nonreciprocity.—The electromagnetic response is nonreciprocal when $\chi_{ij}(\omega) \neq \chi_{ji}(\omega)$. For the static response generally $\chi_{ij}(0) = \chi_{ji}(0)$ for any ABS system, since the equilibrium current $J^i_{\mathrm{eq}} = (2e/\hbar)\partial_{\varphi_i} F$ in lead i is a derivative of the free energy versus the electromagnetic phase $\varphi_i/2 = eV_i/(-i\hbar\omega)$ of that lead. Hence the susceptibility

$$\chi_{ij}(0) = \chi_{ji}(0) = (L^{-1})_{ij} = \frac{4e^2}{\hbar^2}\frac{\partial^2 F}{\partial\varphi_i \partial\varphi_j} \quad (2)$$

is the inverse Josephson inductance matrix L^{-1}. [23].

According to Eq. (1) the situation is different for $\omega > 0$, and the response can be nonreciprocal if

$$\mathrm{Im} I^i_{kk'} I^j_{k'k} \neq 0 \quad (3)$$

for some leads $i \neq j$ and ABS $k \neq k'$. Indeed, for $\omega \ll |\epsilon_k - \epsilon_{k'}|$ and $T = 0$, Eq. (1) becomes, [24,25] using $\hbar I^i_{kk'}/e = (\epsilon_k - \epsilon_{k'})\langle k|\partial_{\varphi_i}|k'\rangle - \delta_{kk'}\partial_{\varphi_i}\epsilon_k$,

$$\chi_{ij}^{\mathrm{ABS}}(\omega) \simeq \chi_{ij}^{\mathrm{ABS}}(0) - 2i\omega\frac{e^2}{\hbar}\sum_{\epsilon_k>0} B^k_{ij}. \quad (4)$$

The low-frequency nonreciprocal part consists of the ABS Berry curvatures $B^k_{ij} = -B^k_{ji} = -2\mathrm{Im}[(\partial_{\varphi_i}\langle k|)\partial_{\varphi_j}|k\rangle]$, which is accessible in microwave experiments [26]. The maximal nonreciprocity is, however, usually not reached in this regime.

For time-reversed states $\bar{k}$, $\bar{k}'$ we have $I^i_{\bar{k}\bar{k}'} I^j_{\bar{k}'\bar{k}} = (I^i_{kk'} I^j_{k'k})^*$. Hence, time-reversal symmetry $\epsilon_{\bar{k}} = \epsilon_k$ generally cancels the nonreciprocal contribution. Moreover, spatial (permutation of leads) symmetry also prevents it. Nonzero superconducting phase differences $\varphi_i \neq \varphi_j$ between leads lift both symmetries, and are generically sufficient to generate nonreciprocal ABS response.

For typical superconducting systems flux bias is then usually needed. However, systems with "intrinsic flux biasing" do exist: they are the systems featuring φ_0 [15–17] and superconducting diode effects [1–12]. They break the time reversal symmetry and hence are likely to also support nonreciprocal rf response without external flux bias.

Scattering approach.—To pose a minimal model where ABS energies and matrix elements are easy to find, we use the scattering approach [27,28]. The technical details are as follows. The Bogoliubov–de Gennes (BdG) equation in each of the leads i can be written as $\mathcal{H}_i\phi_i = \epsilon\phi_i$, where in the Andreev approximation, at $x < 0$,

$$\mathcal{H}_i = v\gamma_3[\hat{k}_x + q_i\tau_3 + A_i(x)\tau_3] + \Delta\tau_1\gamma_1. \quad (5)$$

Here and below we use units with $e = \hbar = 1$. The basis here is $\phi = (\phi^e_+; \phi^h_-; \phi^e_-; \phi^h_+) = (\phi_>; \phi_<)$ corresponding to the wave function $\psi^{e/h}(x) = \sum_\pm \phi^{e/h}_\pm(x) e^{\pm i k_F x}$, where $\phi^{e/h}_\pm$ are vectors containing the coefficients for the different leads, spin, and scattering channels. Here $\tau_j = 1 \otimes \sigma_j$ and $\gamma_j = \sigma_j \otimes 1$ are Pauli matrices in the Nambu e/h and group velocity $> / <$ spaces, q_i is the superfluid momentum in each lead, and $A(x)$ is the vector potential. The junction at $x > 0$ is characterized by the scattering matrix S boundary condition $\phi_<(0) = S\phi_>(0)$, and Andreev reflection in Eq. (5) results to $\phi_>(0) = S_A(\epsilon_k)\phi_<(0)$. Here,

$$S = \begin{pmatrix} S_e & 0 \\ 0 & S_h \end{pmatrix}, \qquad S_A = \begin{pmatrix} 0 & a_+ \\ a_- & 0 \end{pmatrix}, \quad (6)$$

and $a_\pm = \exp\{-i\arccos[(\epsilon \mp vq)/\Delta]\}$. The superconducting phases of the leads are contained in S, $S^{ij}_{e/h} = e^{\pm i(\varphi_i - \varphi_j)/2}(S^{(0)}_{e/h})^{ij}$. The BdG current operator in lead i is $\hat{J}^i = -\frac{1}{2}\partial\mathcal{H}/\partial A = -\frac{1}{2}v\gamma_3\tau_3 P_i$, where P_i is a projector to the channels in lead i, and the factor $\frac{1}{2}$ accounts for BdG double counting of states. For $q = 0$ the bound states can be solved [24,28] via the eigenproblem $S_e S_h w_k = e^{i\alpha_k} w_k$, which gives $\epsilon_k = \Delta\cos(\alpha_k/2)$ with $0 \le \alpha_k \le 2\pi$. The corresponding ABS wave function vector at the interface is

$$\phi^k(0) = N_k(e^{i\alpha_k/2} S_e^\dagger w_k; w_k; e^{i\alpha_k/2} w_k; S_h w_k), \quad (7)$$

where $N_k = (\Delta^2 - \epsilon_k^2)^{1/4}/(2v w_k^\dagger w_k)^{1/2}$ is the normalization constant. We neglect self-consistency in the leads, and evaluate the current at the interface, $I^i_{kk'} = \phi^k(0)^\dagger \hat{J}^i \phi^{k'}(0)$. Then Eq. (1) follows via standard methods [29].

Equation (1) captures the bound-state part of the response properly, but obtaining the continuum response from it would need more care. It is more convenient to use the corresponding Green's function expression [29]

$$\chi_{ij}(\omega) = \int_{-\infty}^{\infty} \frac{d\epsilon}{i\pi} \mathrm{tr}[\hat{J}^i G^>_\epsilon \hat{J}^j G^{A-}_{\epsilon-\omega} + \hat{J}^i G^{R+}_\epsilon \hat{J}^j G^>_{\epsilon-\omega}]. \quad (8)$$

Here, $G^>_\epsilon = (G^R_\epsilon - G^A_\epsilon) f(-\epsilon)$ is the equilibrium Green's function, and $G^{R/A,+}_\epsilon = G^+(\epsilon \pm i0^+)$, [35] where

$$G^+(\epsilon) = -i\begin{pmatrix} 1 \\ S \end{pmatrix}[1 - S_A(\epsilon)S]^{-1}\begin{pmatrix} 1 & S_A(\epsilon) \end{pmatrix} v^{-1}. \quad (9)$$

This result for $G^+(\epsilon) = G(x = 0, x' = 0^-, \epsilon)$ is found by solving the equation $[\epsilon - \mathcal{H}]G(x, x') = \delta(x - x')$ with the S boundary condition at $x = 0$ and boundedness at $x \to -\infty$.

Also, $G^-(\epsilon) = G(x = 0^-, x' = 0, \epsilon) = G^+(\epsilon) + i\gamma_3 v^{-1}$. Equation (8) is the first-order correction from the perturbation series $G = G_0 - G_0 A \hat{J} G_0 + \cdots$ to $J^i = -i\mathrm{tr}\hat{J}^i G^>$.

Nonreciprocity in a fully symmetric junction.—To illustrate the formation of the nonreciprocity in a simple model, let us consider the response in a symmetric three-terminal single-channel junction. The most general scattering matrix invariant with swapping the leads is

$$S_e = e^{i\phi}\begin{pmatrix} 1+c & c & c \\ c & 1+c & c \\ c & c & 1+c \end{pmatrix}, \qquad S_h = S_e^*, \tag{10}$$

where ϕ is an irrelevant overall phase, and $c = -\frac{2}{3}e^{i\gamma}\cos\gamma$ where γ is a real parameter describing the transmission amplitude between the leads. This form assumes spin-rotation invariance, so the spin sector is trivial.

The ABS energy is $\epsilon_1 = \Delta\sqrt{1+\cos^2(\gamma)(|d|^2-1)}$, where $d = \frac{1}{3}\sum_{j=1}^3 e^{i\varphi_j}$. The energy is closest to zero at $d = 0$, i.e., $(\varphi_1, \varphi_2, \varphi_3) = (0, 2\pi/3, -2\pi/3)$, as illustrated in Fig. 1(b). At this point, the additional symmetry allows diagonalization with $w_k = (1, e^{i\zeta_k}, e^{-i\zeta_k})/\sqrt{3}$, $\zeta_k = \pm(\pi/3), \pi$. The only nonzero current operator matrix elements are $I^i_{1,-1} = (I^i_{-1,1})^* = (\Delta\cos^2\gamma/3)e^{i\eta_i - i\gamma}$, $\eta_i = 0, -2\pi/3, 2\pi/3$, for $0 \le \gamma \le \pi/2$. From Eq. (1), accounting for spin and at zero temperature,

$$\chi^{\mathrm{ABS}}_{ij}(\omega) = \frac{4\Delta^2\cos^4\gamma}{9}\sum_{\pm}\frac{\pm e^{\pm i(\eta_i-\eta_j)}}{\omega + i0^+ \mp 2\epsilon_1}, \tag{11}$$

and $\epsilon_1 = \Delta\sin\gamma$. The ABS response at this flux configuration is clearly nonreciprocal, $\chi_{ij} \neq \chi_{ji}$. As the underlying normal-state scattering matrix is otherwise fully symmetric, it is clear flux biasing is then fairly generally sufficient for the nonreciprocity.

Moreover, this nonreciprocity is generated by superconductivity: in the normal state $\Delta \to 0$ from Eq. (8) we find the scattering theory relation [36] $\chi_{ij}(\omega) = -i\omega Y_{ij}$, $Y_{ij} = (1/2\pi)\mathrm{tr}[P_i\delta_{ij} - (S_e^{ij})^\dagger S_e^{ij}]$ between the multiterminal scattering matrix and the ohmic conductance matrix Y. It is here fully reciprocal. In the normal state, Y is independent of the flux biasing of the leads.

The nonreciprocal part $\chi^{\mathrm{nr}} = (\chi - \chi^T)/2$ from Eq. (11) is shown in Fig. 2(a). The real part $\mathrm{Re}\chi^{\mathrm{nr}}$ describes dissipative response, and the imaginary part $\mathrm{Im}\chi^{\mathrm{nr}}$ is reactive. The ABS pair-breaking resonance, $\chi^{\mathrm{nr}}_{21} \sim iA(\{\varphi\})\Delta/(\omega - 2\epsilon_1(\{\varphi\}) + i0^+)$, dominates up to the frequency $\omega = \Delta + \epsilon_1$ where transitions involving the continuum spectrum activate. Phase dependence of the resonance weight A is shown in Fig. 2(b).

The above results correspond to the $T = 0$ ground state. Quasiparticle poisoning can significantly modify the linear response. [29,37] From Eq. (1), in the poisoned state one expects the ABS resonance to be either absent in the spin-rotation symmetric case, or shifted in frequency otherwise.

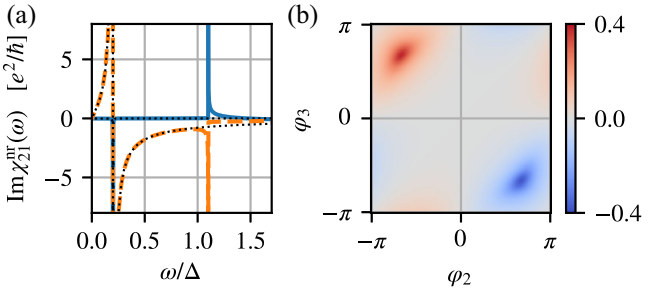

FIG. 2. (a) Elements of the nonreciprocal response coefficient $\chi^{\mathrm{nr}}_{ij}(\omega) = [\chi_{ij}(\omega) - \chi_{ji}(\omega)]/2$ of the symmetric three-terminal junction, for $\gamma = 0.1$ at $(\varphi_1, \varphi_2, \varphi_3) = (0, 2\pi/3, -2\pi/3)$. The real (solid) and imaginary (dashed) parts from Eq. (8) are shown, in addition to Eq. (11) (dotted). (b) Resonance weight $A(\{\varphi\})$ in χ^{nr}_{21} for $\{\varphi\} = (0, \varphi_2, \varphi_3)$.

Multichannel systems.—The nonreciprocity from flux biasing is sensitive to phase shifts in the current operator matrix elements, which can depend on microscopic details. In Fig. 3(a) we show numerical evidence for its scaling with the number of channels $N_>$ in each lead, for random time-reversal symmetric S [28,38] with flux biasing. The mean value $\langle\langle\hat{\chi}^{\mathrm{nr}}\rangle\rangle$ is zero, in contrast to the reciprocal part $\langle\langle\hat{\chi}^{\mathrm{r}}\rangle\rangle$ which scales linearly with $N_>$. The variance is similar for the reciprocal and nonreciprocal parts, and it is constant at ω below the ABS gap, $\omega < \min|\epsilon_k|$, and proportional to

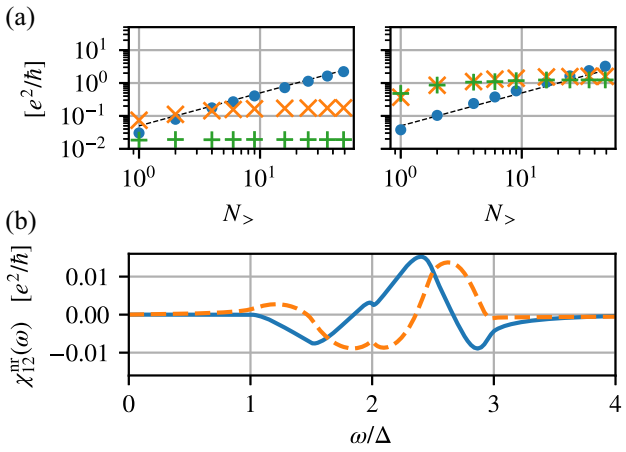

FIG. 3. (a) Susceptibility in multichannel systems. Mean $\langle\langle\mathrm{Re}\hat{\chi}^{\mathrm{r}}_{12}\rangle\rangle$ (circle) and standard deviation $\langle\langle(\mathrm{Re}\delta\hat{\chi}^{\mathrm{r}}_{12})^2\rangle\rangle^{1/2}$ (×), $\langle\langle(\mathrm{Im}\delta\hat{\chi}^{nr}_{12})^2\rangle\rangle^{1/2}$ (+) of reactive susceptibility (linewidth $\Gamma = 10^{-3}\Delta$) vs channel count $N_>$, averaged over 10^5 circular orthogonal ensemble $S^{(0)}$ [28,38], and $\varphi_i = (0, \pi/3, -2\pi/3)$. Dashed line indicates linear scaling. Left panel: below ($\omega = 0.05\Delta$), and right panel: above ($\omega = 0.3\Delta$) lowest ϵ_k. (b) Elements of the nonreciprocal response coefficient $\chi^{\mathrm{nr}}_{ij}(\omega)$ of the symmetric 3-probe system at $\varphi_i \approx (0, 0.323, -0.323)$ for $vq_i = (0, 0.5\Delta, -0.5\Delta)$ and $\gamma = \pi/4$. Dissipative (solid) and reactive (dashed) parts are shown.

inverse ABS linewidth Γ^{-1} above it [39]. Hence, we expect a typical diffusive system without spin-orbit interaction to exhibit flux-driven nonreciprocal susceptibility, even if geometrically symmetric in the normal state, but potentially with a random sign.

Nonreciprocity without flux bias.—Consider then situations where the nonreciprocity does not require flux biasing. At equilibrium the superconducting phases φ_i minimize the junction free energy $F = -2T\sum_{n=0}^{\infty} \mathrm{Re}\ln\det[1 - S_A(i\omega_n)S]$, where $\omega_n = 2\pi T(n+\frac{1}{2})$. In systems with a φ_0 effect [15–17], this configuration can have $\varphi_i \neq 0, \pm\pi$ and nonzero nonreciprocity. Moreover, nonreciprocity in the scattering matrix S is also inherited by the superconducting system.

As a simple example of the nonreciprocity of normal-state scattering, consider a chiral three-probe junction,

$$S_e = \begin{pmatrix} 0 & 1 & 0 \\ 0 & 0 & 1 \\ 1 & 0 & 0 \end{pmatrix}, \qquad \chi_{ij}^{\mathrm{ABS}}(\omega) = \frac{\Delta^2}{8}\sum_{\pm}\frac{\pm e^{\pm i(\eta_i - \eta_j)}}{\omega + i0^+ \mp \Delta}, \tag{12}$$

where $\eta_i = (7\pi/6, 11\pi/6, \pi/2)$. This system has an ABS pinned at $\epsilon_k = \pm\Delta/2$ and no equilibrium supercurrent, but the ABS contribute a nonreciprocal response independent of the flux biasing, reflecting broken time-reversal symmetry of the normal state.

For the φ_0 effect and nonreciprocity without normal-state asymmetry or flux biasing, we consider a model proposed in Ref. [5] for a superconducting diode. There, the effects are induced by a screening current superflow $vq_i \neq 0$ in the leads.

In Fig. 3(b) we show the nonreciprocal part of the susceptibility from Eq. (8) for the symmetric 3-probe system with $vq_i \neq 0$. The equilibrium phase differences are nonzero, indicating the φ_0 effect induced by the superflow. Here the phase differences are small, and ABS remains embedded in the continuum at $|\epsilon| > \Delta - vq$, and couples less strongly to the electromagnetic response. Other realizations of the φ_0 effect such as the one combining spin-orbit interaction and spin splitting [8] are likely to exhibit stronger nonreciprocity at lower frequencies.

Scattering parameters.—For many applications, the interesting quantity are the electromagnetic transmission line scattering parameters $\mathcal{S}_{ij}$, which indicate the amplitude and phase of the rf signal output from port i generated by input in port j (as in Fig. 1). It is related to the admittance matrix $Y_{ij}(\omega) = \chi_{ij}(\omega)/(i\omega)$ by [42]

$$\mathcal{S}(\omega) = \frac{1 - \mathcal{Z}^{1/2}Y(\omega)\mathcal{Z}^{1/2}}{1 + \mathcal{Z}^{1/2}Y(\omega)\mathcal{Z}^{1/2}}, \tag{13}$$

where $\mathcal{Z} = \mathrm{diag}(Z_1, \ldots, Z_N)$ is a diagonal matrix containing the characteristic impedances of transmission lines

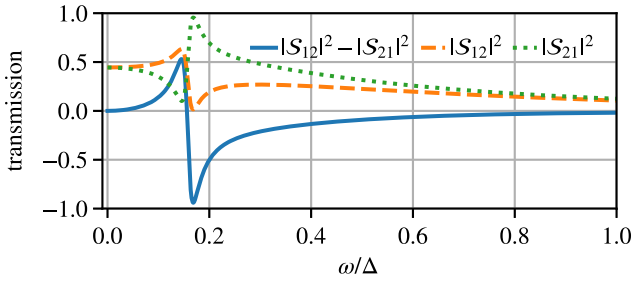

FIG. 4. Nonreciprocity of the electromagnetic transmission through the flux-biased symmetric three-terminal junction, for $\gamma = 0.1$ at $(\varphi_1, \varphi_2, \varphi_3) = (0, 2\pi/3, -2\pi/3)$, and lead characteristic impedances $Z_i \approx 80\Omega$. Flux bias loop inductances are assumed to be $L_L = \hbar^2/(10e^2\Delta)$.

connected to each terminal i. If χ is nonreciprocal, then generally also $\mathcal{S}$ is. At low frequency, $Y(\omega) \simeq L/(-i\omega) + Y^{\mathrm{nr}}(0)$ where Y^{nr} is the nonreciprocal part, so that $\mathcal{S}^{\mathrm{nr}} = \frac{1}{2}(\mathcal{S} - \mathcal{S}^T) \simeq 2\omega^2\mathcal{Z}^{1/2}LY^{\mathrm{nr}}L\mathcal{Z}^{1/2}$. The nonreciprocal contribution, which for $\omega \to 0$ contains the ABS Berry curvature, [24] can be accessed in the scattering experiment, in absorption [26] and as seen above also in the reactive response.

The largest nonreciprocal response does not generically occur in the low-frequency limit. Maximally nonreciprocal admittance is obtained in the high-transparency limit $\gamma \to 0$ at $\varphi_i = (0, 2\pi/3, -2\pi/3)$, where $\epsilon_k \to 0$ and

$$Y^{\mathrm{ABS}} = \frac{e^2}{\hbar}\frac{4\sqrt{3}\Delta^2}{9\omega^2}\begin{pmatrix} 0 & -1 & 1 \\ 1 & 0 & -1 \\ -1 & 1 & 0 \end{pmatrix}, \tag{14}$$

which is reactive and nonreciprocal. This expression assumes $\omega \gg \epsilon_k, \Gamma$, where Γ is the ABS linewidth. Flux biasing to this working point is possible with three bias loops (see Fig. 1) with inductance L_L such that $\hbar^2/(e^2L_L\Delta) > 2|\cos\gamma\cot\gamma|/9$ [29]. They contribute admittance $Y_{ij}^L = (1/-i\omega L_L)(3\delta_{ij} - 1)$, so that $Y = Y^{\mathrm{ABS}} + Y^L$. The resulting $\mathcal{S}$ is illustrated in Fig. 4, where the large nonreciprocal peak comes from the ABS contribution. The peak occurs where $\mathcal{Z}Y_{\mathrm{ABS}} \sim 1$, which for the parameters here is close but not exactly at the ABS resonance. $\mathcal{S}$ is nonunitary at $\omega > \epsilon_k + \Delta$ and at the resonant frequency $\omega = 2\epsilon_k$, which can be separated from the peak nonreciprocity. The exact peak shape and height depends on the details of impedance matching, and with suitable Z_i it is possible to reach $||S_{12}|^2 - |S_{21}|^2| \approx 1$.

Conclusions.—Although the static electromagnetic response of Josephson junctions is always reciprocal, at any nonzero frequency it generically becomes nonreciprocal if time-reversal symmetry is broken. As the admittance increases around Andreev bound state resonances, this nonreciprocity can be large and provide full transmission

asymmetry matched to transmission lines, even if the response comes from a single bound state.

Multiterminal Josephson junctions with few Andreev bound states have been realized in recent experiments [12,43–45]. In these systems, as shown above, the transmission line scattering parameters are sensitive to the Andreev bound states and at low frequencies their Josephson Berry curvature, and hence provide a way to probe them. In systems with many channels, we expect that the nonreciprocal response has mesoscopic fluctuations, but can be large compared to $e^2/\hbar$ in a typical realization. Moreover, in the presence of strong spin-orbit interaction and exchange field [8], it may be possible to obtain significant nonreciprocity in the absence of flux bias also in multichannel systems. In particular, multiterminal Josephson junctions formed on two-dimensional transition metal dichalcogenides [46] in the presence of either magnetic field or magnetism are interesting candidate systems for observing such effects. The φ_0 and Josephson diode effects have been seen also in twisted bilayer graphene [47,48], making their multiterminal versions also viable candidates for strong flux-free nonreciprocity. There, the nonreciprocal response in the absence of flux bias would be a direct indication of the presence of the φ_0 effect that would have to be otherwise probed with SQUID-based setups or indirectly via Fraunhofer patterns.

As shown by the example in Fig. 4, multiterminal Josephson junctions may be viable candidates for constructing on-chip circulators with strong nonreciprocity and large bandwidth. In conventional superconductors with critical temperature of the order of 1 K, the nonreciprocity would show up in the few GHz regime most relevant for superconducting quantum electronics applications. They can hence form extremely useful components of the emerging quantum technology.

Computer codes used in this Letter are available at [49].

We thank S. Ilić, S. Parkin, P. Hakonen, A. Ronzani, and N. Paradiso for stimulating discussions. This work was supported by the Academy of Finland (Contracts No. 321982 and No. 354735) and the European Union's HORIZON-RIA programme (Grant Agreement No. 101135240 JOGATE).

*pauli.t.virtanen@jyu.fi
†tero.t.heikkila@jyu.fi

[1] J. Hu, C. Wu, and X. Dai, Proposed design of a Josephson diode, Phys. Rev. Lett. **99**, 067004 (2007).
[2] C.-Z. Chen, J. J. He, M. N. Ali, G.-H. Lee, K. C. Fong, and K. T. Law, Asymmetric Josephson effect in inversion symmetry breaking topological materials, Phys. Rev. B **98**, 075430 (2018).
[3] K. Misaki and N. Nagaosa, Theory of the nonreciprocal Josephson effect, Phys. Rev. B **103**, 245302 (2021).
[4] J. J. He, Y. Tanaka, and N. Nagaosa, A phenomenological theory of superconductor diodes, New J. Phys. **24**, 053014 (2022).
[5] M. Davydova, S. Prembabu, and L. Fu, Universal Josephson diode effect, Sci. Adv. **8**, eabo0309 (2022).
[6] N. F. Yuan and L. Fu, Supercurrent diode effect and finite-momentum superconductors, Proc. Natl. Acad. Sci. U.S.A. **119**, e2119548119 (2022).
[7] A. Daido, Y. Ikeda, and Y. Yanase, Intrinsic superconducting diode effect, Phys. Rev. Lett. **128**, 037001 (2022).
[8] S. Ilić and F. S. Bergeret, Theory of the supercurrent diode effect in Rashba superconductors with arbitrary disorder, Phys. Rev. Lett. **128**, 177001 (2022).
[9] F. Ando, Y. Miyasaka, T. Li, J. Ishizuka, T. Arakawa, Y. Shiota, T. Moriyama, Y. Yanase, and T. Ono, Observation of superconducting diode effect, Nature (London) **584**, 373 (2020).
[10] C. Baumgartner, L. Fuchs, A. Costa, S. Reinhardt, S. Gronin, G. C. Gardner, T. Lindemann, M. J. Manfra, P. E. Faria Junior, D. Kochan *et al.*, Supercurrent rectification and magnetochiral effects in symmetric Josephson junctions, Nat. Nanotechnol. **17**, 39 (2022).
[11] H. Wu, Y. Wang, Y. Xu, P. K. Sivakumar, C. Pasco, U. Filippozzi, S. S. Parkin, Y.-J. Zeng, T. McQueen, and M. N. Ali, The field-free Josephson diode in a van der Waals heterostructure, Nature (London) **604**, 653 (2022).
[12] M. Gupta, G. V. Graziano, M. Pendharkar, J. T. Dong, C. P. Dempsey, C. Palmstrøm, and V. S. Pribiag, Gate-tunable superconducting diode effect in a three-terminal Josephson device, Nat. Commun. **14**, 3078 (2023).
[13] J. Chiles, E. G. Arnault, C.-C. Chen, T. F. Q. Larson, L. Zhao, K. Watanabe, T. Taniguchi, F. Amet, and G. Finkelstein, Nonreciprocal supercurrents in a field-free graphene Josephson triode, Nano Lett. **23**, 5257 (2023).
[14] A. Andreev, Electron spectrum of the intermediate state of superconductors, Sov. Phys. JETP **22**, 455 (1966).
[15] I. V. Krive, A. M. Kadigrobov, R. I. Shekhter, and M. Jonson, Influence of the Rashba effect on the Josephson current through a superconductor/Luttinger liquid/superconductor tunnel junction, Phys. Rev. B **71**, 214516 (2005).
[16] A. Buzdin, Direct coupling between magnetism and superconducting current in the Josephson φ_0 junction, Phys. Rev. Lett. **101**, 107005 (2008).
[17] F. Konschelle, I. V. Tokatly, and F. S. Bergeret, Theory of the spin-galvanic effect and the anomalous phase shift φ_0 in superconductors and Josephson junctions with intrinsic spin-orbit coupling, Phys. Rev. B **92**, 125443 (2015).
[18] K. M. Sliwa, M. Hatridge, A. Narla, S. Shankar, L. Frunzio, R. J. Schoelkopf, and M. H. Devoret, Reconfigurable Josephson circulator/directional amplifier, Phys. Rev. X **5**, 041020 (2015).
[19] S. Barzanjeh, M. Wulf, M. Peruzzo, M. Kalaee, P. Dieterle, O. Painter, and J. M. Fink, Mechanical on-chip microwave circulator, Nat. Commun. **8**, 953 (2017).
[20] N. Trivedi and D. A. Browne, Mesoscopic ring in a magnetic field: Reactive and dissipative response, Phys. Rev. B **38**, 9581 (1988).
[21] F. Chiodi, M. Ferrier, K. Tikhonov, P. Virtanen, T. T. Heikkilä, M. Feigelman, S. Guéron, and H. Bouchiat,

Probing the dynamics of Andreev states in a coherent normal/superconducting ring, Sci. Rep. **1**, 3 (2011).
[22] M. Ferrier, B. Dassonneville, S. Guéron, and H. Bouchiat, Phase-dependent Andreev spectrum in a diffusive SNS junction: Static and dynamic current response, Phys. Rev. B **88**, 174505 (2013).
[23] The sum rule for obtaining Eq. (2) from the Kubo formula involves continuum states in addition to the ABS.
[24] R.-P. Riwar, M. Houzet, J. S. Meyer, and Y. V. Nazarov, Multi-terminal Josephson junctions as topological matter, Nat. Commun. **7**, 11167 (2016).
[25] E. V. Repin, Y. Chen, and Y. V. Nazarov, Topological properties of multiterminal superconducting nanostructures: Effect of a continuous spectrum, Phys. Rev. B **99**, 165414 (2019).
[26] R. L. Klees, G. Rastelli, J. C. Cuevas, and W. Belzig, Microwave spectroscopy reveals the quantum geometric tensor of topological Josephson matter, Phys. Rev. Lett. **124**, 197002 (2020).
[27] C. W. J. Beenakker, Universal limit of critical-current fluctuations in mesoscopic Josephson junctions, Phys. Rev. Lett. **67**, 3836 (1991).
[28] C. W. J. Beenakker, Random-matrix theory of quantum transport, Rev. Mod. Phys. **69**, 731 (1997).
[29] See Supplemental Material at http://link.aps.org/supplemental/10.1103/PhysRevLett.132.046002 for intermediate steps, including Refs. [30–34].
[30] J. S. Meyer and M. Houzet, Nontrivial Chern numbers in three-terminal Josephson junctions, Phys. Rev. Lett. **119**, 136807 (2017).
[31] F. S. Bergeret, P. Virtanen, T. T. Heikkilä, and J. C. Cuevas, Theory of microwave-assisted supercurrent in quantum point contacts, Phys. Rev. Lett. **105**, 117001 (2010).
[32] F. Kos, S. E. Nigg, and L. I. Glazman, Frequency-dependent admittance of a short superconducting weak link, Phys. Rev. B **87**, 174521 (2013).
[33] A. Zazunov, A. Brunetti, A. L. Yeyati, and R. Egger, Quasiparticle trapping, Andreev level population dynamics, and charge imbalance in superconducting weak links, Phys. Rev. B **90**, 104508 (2014).
[34] A. Schmid, Diffusion and localization in a dissipative quantum system, Phys. Rev. Lett. **51**, 1506 (1983).
[35] Nonzero ABS linewidth Γ can be included by replacing $\epsilon \pm i0^+ \mapsto \epsilon \pm i\Gamma/2$, corresponding to a model where the leads are coupled to normal-state quasiparticle sinks.
[36] Y. A. Blanter and M. Büttiker, Shot noise in mesoscopic conductors, Phys. Rep. **336**, 1 (2000).
[37] C. Janvier, L. Tosi, L. Bretheau, Ç. Ö. Girit, M. Stern, P. Bertet, P. Joyez, D. Vion, D. Esteve, M. F. Goffman, H. Pothier, and C. Urbina, Coherent manipulation of Andreev states in superconducting atomic contacts, Science **349**, 1199 (2015).
[38] M. L. Mehta, *Random Matrices* (Elsevier, New York, 2004).
[39] A similar linewidth dependence occurs in another mesoscopic fluctuation effect, universal conductance fluctuations in an isolated system where electrons cannot relax to the electrodes [40,41].
[40] R. A. Serota, S. Feng, C. Kane, and P. A. Lee, Conductance fluctuations in small disordered conductors: Thin-lead and isolated geometries, Phys. Rev. B **36**, 5031 (1987).
[41] R. A. Serota, Fluctuations of ultrasonic attenuation in mesoscopic systems: A test for isolated geometries, Phys. Rev. B **38**, 12640 (1988).
[42] R. E. Collin, *Foundations for Microwave Engineering* (Wiley, New York, 2001).
[43] N. Pankratova, H. Lee, R. Kuzmin, K. Wickramasinghe, W. Mayer, J. Yuan, M. G. Vavilov, J. Shabani, and V. E. Manucharyan, Multiterminal Josephson effect, Phys. Rev. X **10**, 031051 (2020).
[44] M. Coraiola, D. Z. Haxell, D. Sabonis, H. Weisbrich, A. E. Svetogorov, M. Hinderling, S. C. ten Kate, E. Cheah, F. Krizek, R. Schott, W. Wegscheider, J. C. Cuevas, W. Belzig, and F. Nichele, Phase-engineering the Andreev band structure of a three-terminal Josephson junction, Nat. Commun. **14**, 6784 (2023).
[45] E. G. Arnault, T. F. Q. Larson, A. Seredinski, L. Zhao, S. Idris, A. McConnell, K. Watanabe, T. Taniguchi, I. Borzenets, F. Amet, and G. Finkelstein, Multiterminal inverse ac Josephson effect, Nano Lett. **21**, 9668 (2021).
[46] L. Bauriedl, C. Bäuml, L. Fuchs, C. Baumgartner, N. Paulik, J. M. Bauer, K.-Q. Lin, J. M. Lupton, T. Taniguchi, K. Watanabe *et al.*, Supercurrent diode effect and magneto-chiral anisotropy in few-layer $NbSe_2$, Nat. Commun. **13**, 4266 (2022).
[47] J. Diez-Merida, A. Diez-Carlon, S. Y. Yang, Y. M. Xie, X. J. Gao, K. Watanabe, T. Taniguchi, X. Lu, K. T. Law, and D. K. Efetov, Magnetic Josephson junctions and superconducting diodes in magic angle twisted bilayer graphene, arXiv:2110.01067.
[48] J. Díez-Mérida, A. Díez-Carlón, S. Yang, Y.-M. Xie, X.-J. Gao, J. Senior, K. Watanabe, T. Taniguchi, X. Lu, A. P. Higginbotham *et al.*, Symmetry-broken Josephson junctions and superconducting diodes in magic-angle twisted bilayer graphene, Nat. Commun. **14**, 2396 (2023).
[49] P. Virtanen Nonreciprocal Josephson linear response (parent repository), V. 22.6.2023, University of Jyväskylä (2023) 10.17011/jyx/dataset/88359.